NUMERICAL EVALUATION OF SEISMIC PERFORMANCE OF REINFORCED CONCRETE BRIDGE PIERS USING DYNAMIC LATTICE MODEL

(Translation from Proceedings of JSCE, No.704/V-55, pp.151-161, May 2002)

Tomohiro MIKI

Junichiro NIWA

Manakan LERTSAMATTIYAKUL

This paper describes a procedure for evaluating the seismic performance of reinforced concrete bridge piers under earthquake motion. The evaluation is carried out with a newly developed computer program using the lattice model, an analytical model used to derive changes in the shear-resisting mechanism. The results obtained using this lattice model are compared with several sets of experimental results, including static reversed cyclic loading tests and shaking table tests. Based on these comparisons, the applicability of static and dynamic lattice models to the prediction of the static cyclic behavior and seismic response of RC bridge piers is demonstrated. Of additional note is that the influence of transverse reinforcement on seismic performance can be properly estimated in terms of the energy absorbed by RC bridge piers.

Keywords: *reinforced concrete bridge piers, seismic performance, non-linear dynamic analysis, lattice model*

Tomohiro Miki is a graduate student in the Department of Civil Engineering at Graduate School of Tokyo Institute of Technology. His research interests relate to the nonlinear analysis of RC structure using the lattice model and the numerical evaluation of seismic performance of reinforced concrete bridge piers.

Junichiro Niwa is a professor in the Department of Civil Engineering at Graduate School of Tokyo Institute of Technology. He received his Doctor of Engineering degrees from the University of Tokyo. He specializes in the mechanics of concrete structures including fracture mechanics and nonlinear numerical analysis. He is a member of JSCE, JCI, IABSE, fib, and ACI.

Manakan Lertsamattiyakul is a graduate student in the Department of Civil Engineering at Graduate School of Tokyo Institute of Technology. His research interests the shear analysis for D-region in RC PC structural members.

1. INTRODUCTION

The Hyogo-ken Nanbu Earthquake presented an opportunity for extensive revision of the standard specifications for the seismic design of concrete structures. The updated standard specifications are based on the concept that considerable inelastic deformation can be permitted after the longitudinal reinforcement yields, rather than considering only elastic behavior, for concrete structures subjected to large ground motions. A series of revisions to the standard specifications was carried out with respect to the design of reinforced concrete (RC) bridge piers for highway bridges, with ductility design adopted to take into consideration the deformation capacity of such structures. It is also specified that designers must perform verification using dynamic analysis taking into account the nonlinearity of the concrete members.

At present, this dynamic analysis is generally based on the frame model or the fiber model [1], which can simulate the mechanical behavior of RC piers in the nonlinear response region. With the frame model, the RC structure is modeled into individual RC members that incorporate restoring characteristics. On the other hand, with the fiber model, a RC member is discretized longitudinally into several layers in which the layer is subdivided into some fiber element. Each element consists of uniaxial fibers so that its stress-strain relationship is properly incorporated.

These methods are recognized as a highly practical method of evaluating the plastic deformation behavior of flexural RC structures. However, it is necessary to idealize the location and size of the plastic hinge region and incorporate it into the appropriate fiber element. Moreover, one shortcoming of these models is the relative difficulty in estimating behavior in the post-peak range, particularly when the failure mode of the RC member is shear.

In this study, these methods are replaced by the lattice model [2]. This model offers reasonable prediction of the shear-carrying capacity of RC members, making it a significant departure from analytical methods based on fiber techniques. Moreover, since the lattice model discretizes an RC member into truss elements, internal stress flows can easily be determined. From an understanding of the internal resistance mechanism of RC members, the accuracy of analytical results can be confirmed.

The objective of this study is to develop a dynamic analysis procedure based on the lattice model. First, in order to confirm the performance of the static lattice model under reversed cyclic loading, predictions made with the model are compared with experimental results from laterally loaded RC bridge piers. Next, in order to verify the applicability of the lattice model to dynamic analysis, experimental results from shaking table tests on RC bridge piers are compared. In this comparison, RC bridge piers with identical geometrical arrangements are subject to three magnitudes of input ground acceleration. By comparing the experimental and analytical results, the prediction accuracy of the lattice model in dynamic analysis can be verified and the seismic performance of RC bridge piers subjected to ground motion estimated. Finally, RC bridge piers with different transverse reinforcement ratios are simulated. On the basis of these predictions, the effect of transverse reinforcement ratio on seismic performance is estimated through dynamic lattice model analysis.

2. ANALYTICAL MODEL

2.1 Outline of lattice model

The lattice model consists of members representing both concrete and reinforcement, as schematically shown in **Fig. 1**. The concrete is modeled into flexural compression members, flexural tension members, diagonal compression members, diagonal tension members, vertical members and an arch member. The longitudinal and transverse reinforcement are modeled into horizontal and vertical members, respectively.

The truss action of shear resistance is represented in the lattice model by diagonal compression members and diagonal tension members. These are placed in a regular arrangement with inclination angles of 45° and 135° to the longitudinal axis of the model, respectively.

By incorporating an arch member to represent arch action, the lattice model can be used to estimate the changing direction of internal compressive stress flows after diagonal cracking. The arch member is modeled as a connection between the loading and support points, as depicted in **Fig. 1**. It should be noted that, for appropriate estimation of the shear carrying mechanism of RC members, the location of the arch member is comparatively important.

2.2 Modeling of each element

A schematic diagram of the cross section of an RC member in the lattice model is shown in **Fig. 2**. The web concrete is divided into truss and arch components. When the value of "t" is defined as the ratio of the width of the arch part to the width of cross section "b", the widths of the arch and truss parts are given as bt and b(1−t), respectively, where $0 < t < 1$. The value of "t" is determined based on the theorem of minimization of total potential energy for the whole member in the initial elastic range.

Pre-analysis is carried out using the lattice model, with the value of "t" varied from 0.05 to 0.95 with a small step of 0.05. The total potential energy can be calculated from the difference between sum of strain energy in each element and the external work. The strain energy is calculated from the stresses and strains of each lattice component produced when the model is subjected to a small displacement at the loading point. This small displacement is fixed as 0.1% of the shear span in this study. It is obvious that, when the structure is subjected to large deformations, significant material nonlinearity is observed and the value of "t" increases with the amount of deformation. In this study, even though the deformation becomes large, the value of "t" as calculated from the initial stiffness is used as an approximate value for simplicity.

Due to the existence of reinforcing bars, the bond effect between concrete and a reinforcing bar becomes a significant factor in the post-peak behavior of the concrete. Further, for flexural tension members with reinforcing bars, the concrete continues to contribute to tensile resistance even after cracking. Consequently, the cross-sectional area of concrete flexural members is, for simplicity, determined by considering the bond effect between concrete and a reinforcing bar, and the cross-sectional area of the flexural tension or compression member is assumed to be equal to the product of twice the concrete cover and the beam width.

2.3 Material models

a) Concrete compression members

It has been confirmed that if a suitable amount of transverse reinforcement is used to confine the concrete, a significant increase in both compressive strength and ductility can be expected. In this study, in order to take into account this confinement effect of transverse reinforcement, the stress-strain relationship ($\sigma_c' - \varepsilon_c'$)

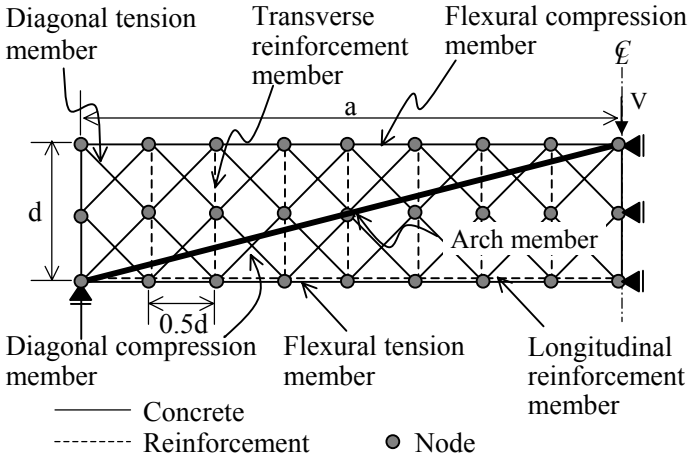

Fig. 1 Concept of the lattice model

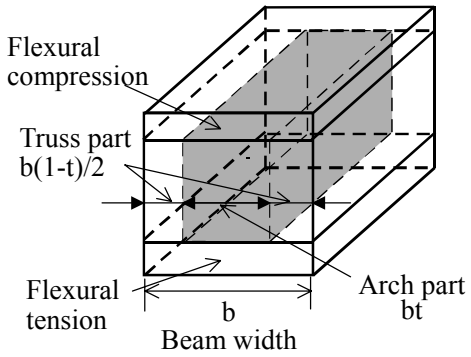

Fig. 2 Cross-section of beam modeled using the lattice model

proposed by Mander, et al. [3] as expressed by Eq. (1) and illustrated in **Fig. 3**, is used as a material model for the diagonal compression members and the arch member.

$$\sigma_c' = \frac{f_{cc}' \cdot x \cdot r}{r - 1 + x^r} \tag{1}$$

where,

$$f_{cc}' = f_c'\left(2.254\sqrt{1 + 7.94 f_l'/f_c'} - 2 f_l'/f_c' - 1.254\right) \quad \text{(in SI Unit)} \tag{2}$$

$$x = \varepsilon_c'/\varepsilon_{cc}' \tag{3}$$

$$\varepsilon_{cc}' = 0.002\left\{1 + 5(f_{cc}'/f_c' - 1)\right\} \tag{4}$$

$$r = E_c/(E_c - E_{\sec}) \tag{5}$$

$$E_c = 5000\sqrt{f_c'} \ \text{(MPa)} \tag{6}$$

$$E_{\sec} = f_{cc}'/\varepsilon_{cc}' \tag{7}$$

$$f_l' = 0.75 \cdot r_w f_{wy} \tag{8}$$

Here, f_c' is the uniaxial compressive strength of the concrete; r_w ($=A_w/b_w s$) is the transverse reinforcement ratio, where A_w is the cross-sectional area of the transverse reinforcement, b_w is the width of the web concrete of the RC member, and s is the transverse reinforcement spacing; and f_{wy} is the yield strength of the transverse reinforcement.

Further, Vecchio and Collins [4] have demonstrated that the ability of diagonally cracked concrete to resist compressive stress decreases as the transverse tensile strain, ε_t, increases, as shown in **Fig. 4**. Therefore, the value of ε_t for the diagonal tension members, which are normal to the diagonal compression members, is used to determine the coefficient of concrete compressive softening, η. The behavior of the cracked concrete in compression is then characterized by Eq. (9). Here, for the arch member, the transverse tensile strain of the diagonal tension member near the loading point is used as the control value.

$$\eta = 1.0/\left\{0.8 - 0.34(\varepsilon_t/\varepsilon_0')\right\} \le 1.0 \tag{9}$$

where, $\varepsilon_0' = -0.002$.

On the other hand, for flexural compression members including the cover concrete, the quadratic stress-strain relationship (Eq. (10)) proposed by Vecchio and Collins [4] is adopted, as illustrated in **Fig. 3**.

$$\sigma_c' = -\eta \cdot f_c'\left\{2(\varepsilon_c'/\varepsilon_0') - (\varepsilon_c'/\varepsilon_0')^2\right\} \tag{10}$$

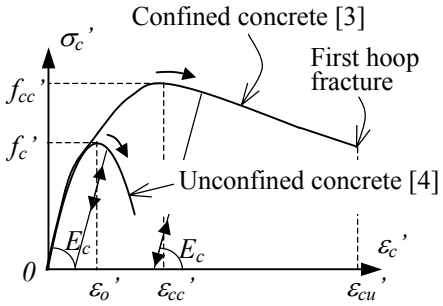

Fig. 3 Compressive stress-strain relationship of concrete

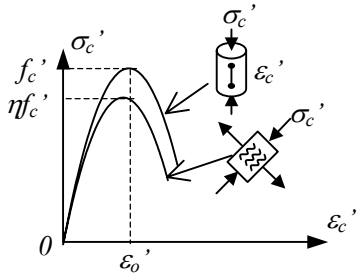

Fig. 4 Reduction in compressive strength of cracked concrete

In the unloading path, the stress is assumed to decrease according to initial stiffness. The reloading curve is assumed to follow the same path as the unloading one. In this study, the decrease in the stiffness due to reversed cyclic loading is not taken into the consideration for simplicity.

b) Concrete tension members

The diagonal tension members exhibit elastic behavior prior to cracking. However, once a crack occurs, the concrete is assumed to exhibit tension softening behavior. In this study, softening behavior, expressed by the 1/4-model [5] shown in **Fig. 5**, is applied to the diagonal tension members. Here, the fracture energy of the concrete, G_F, is assumed to take a standard value of 0.1 N/mm.

Since the flexural tension members contain reinforcing bars, the previously noted bond action takes place between concrete and reinforcing bar, so the concrete continues to sustain tension even after cracking. For the flexural tension members prior to cracking, a linear elastic relationship is applied, while the tension stiffening curve [6] defined by Eq. (11) and illustrated in **Fig 6** is applied after cracking. The strain of crack initiation, ε_{cr}, is assumed to be 0.0001.

$$\sigma_t = f_t\left(\varepsilon_{cr} / \varepsilon_t\right)^{0.4} \tag{11}$$

where, f_t is the uniaxial tensile strength of the concrete.

The unloading path is assumed to fall directly to the origin and the reloading path is assumed to follow the unloading path.

c) Reinforcement

The stress-strain relationship of the reinforcement is modeled as an elasto-plastic expression under monotonic loading. As shown in **Fig. 7**, the stress-strain relationship of the reinforcement is bi-linear, with a tangential stiffness after yielding equal to E_s /100 (where E_s indicates the initial stiffness of the reinforcement). The unloading and reloading paths are also shown in **Fig. 7**. After yield, the stiffness of the reinforcement falls as the stress state moves from tension to compression, while similar behavior is observed when the stress changes from compression to tension. This phenomenon, the so-called Bauschinger effect, is incorporated into the analysis using the model proposed by Fukuura et al. [7]. This is an improved model developed for simplicity in numerical analysis, though it retains the same accuracy as Kato's model [8].

2.4 Nonlinear dynamic analysis procedure

A computer program based on the dynamic lattice model has been newly developed to facilitate the nonlinear dynamic analysis of RC bridge piers. In analysis with the dynamic lattice model, it is assumed that a mass equivalent to the weight of the pier is distributed over all the nodal points. It is also assumed that a concentrated mass equal to the weight of the superstructure acts uniformly on the top of the pier. The numerical procedure implemented in the computer program is explained below.

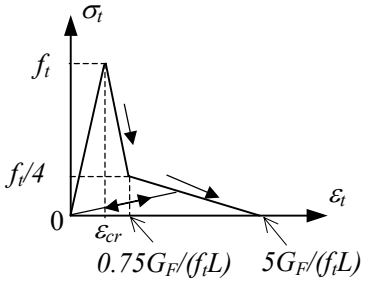

Fig. 5 Tension softening model (1/4 model)

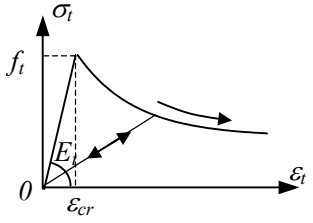

Fig. 6 Tension stiffening model

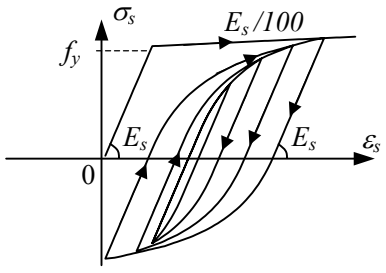

Fig. 7 Stress-strain relationship of reinforcement under cyclic loading

First, an equation of motion satisfying the equilibrium condition for the whole system is formulated. Then, prior to time integration, a change from the nodal displacement of the lattice model to the displacement in the generalized coordinates is performed. The shape of vibration mode is taken as the solution to the free vibration equation, neglecting damping. The vibration mode can be obtained by solving the eigenproblem. In this study, the subspace iteration method is used to obtain this eigenvalue solution.

The stiffness matrix can be obtained from the tangent stiffness considering the concrete and reinforcement nonlinearity. The damping matrix is given in the form of an assumption of the linear combination of the global stiffness matrix and the mass matrix, or so-called Rayleigh damping. By using the procedure as previously mentioned, a system of linear algebraic equations with *n* variables is transferred into *n* equivalent equations, which can then be solved using the direct time integration method. In this study, Newmark's β-method (β=0.25) is employed as the time integration scheme. Finally, by converting back from the generalized displacements to the nodal displacements, the displacement response of the RC structure can be calculated.

Since nonlinear dynamic responses appear when RC structures are subjected to large ground motions, it is necessary to iterate the calculation until a sufficiently converged solution is obtained. The Newton-Raphson iteration method is adopted in this study. Convergence criteria based on both force and energy are used to detect termination. The force criterion is determined from the out-of-balance force, which is equivalent to the difference between the external force and the summation of the inertial force, damping force and restoring force. In addition, the criteria for increments in internal energy during iteration are defined by the amount of work done by the out-of-balance force due to the displacement increment. In this study, the out-of-balance force and the energy increment are compared with initial values during iteration. Here, the convergence tolerances for the out-of-balance force and energy are set at 0.001 and 0.01, respectively.

3. STATIC ANALYSIS OF RC BRIDGE PIERS SUBJECTED TO REVERSED CYCLIC LOADING

3.1 Outlines of experiment

Experimental work carried out by Takemura et al. on RC bridge piers subjected to static reversed cyclic loading [9,10] is adopted as the analytical target. The specimen and reinforcement arrangement are illustrated in **Fig. 8**. Specimen is a cantilever RC bridge pier with a cross section of 400 mm. Reversed cyclic loading was applied by controlled horizontal displacement at a point 1,245 mm above the base of the pier. The material properties of the concrete and reinforcement are summarized in **Table 1**.

In the experiment, the displacement amplitude was increased stepwise in increments of $n\delta_y$ (n = 1, 2, 3…) at each cyclic loading step. Here, δ_y is the lateral displacement at initial yielding of the longitudinal reinforcement at the bottom end of the pier and was taken as δ_y = 6 mm. The cyclic lateral displacement history used in the experiment is shown in **Fig. 9**. Loading hysteresis identical to that in the experiment is obtained in this analysis by using a displacement-controlled incremental calculation. During the test, a constant axial compressive stress of 0.98 MPa was applied at the top of the pier; this is equal to an applied axial compressive load of 156.7 kN.

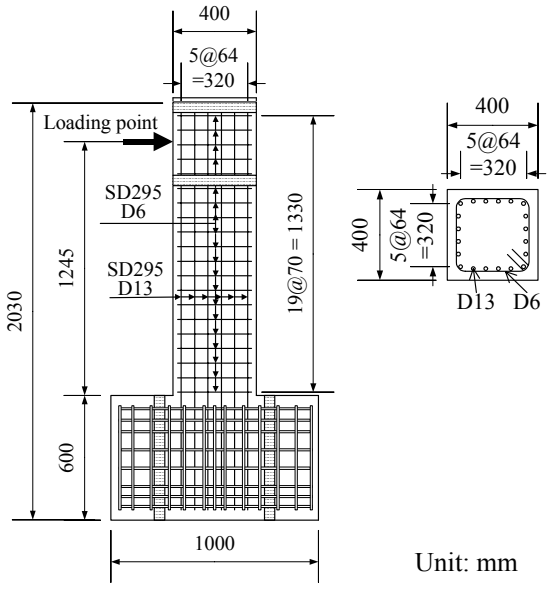

Fig. 8 Specimen details and test setup (static reversed cyclic loading test)

Table 1 Material properties of concrete and reinforcement

Uniaxial compressive strength of concrete, f_c' (MPa)		35.7
Yield strength of reinforcement, f_y (MPa)	SD295 D13	363
	SD295 D6	368

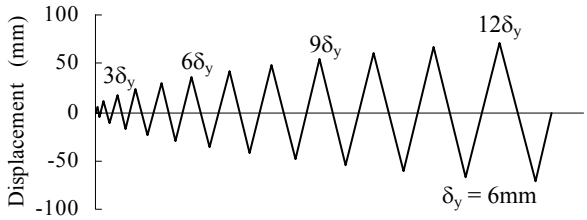

Fig. 9 Cyclic lateral displacement history

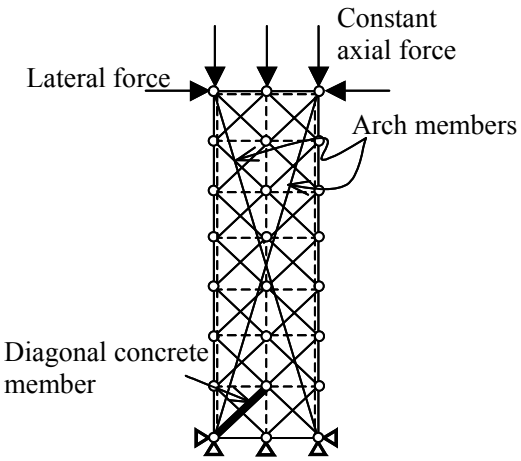

Fig. 10 Static lattice model

In this discussion, loading from the left side of the lattice model, as shown in **Fig. 10**, is defined as positive loading (with lateral force and lateral displacement expressed as positive values). In contrast, loading from the right is defined as negative loading (with lateral force and lateral displacement given as negative values).

3.2 Lattice modeling of specimen

The specimens shown in **Fig. 8** are analyzed by applying an extension of the static lattice model that takes account of the reversed cyclic loading condition [11], as depicted in **Fig. 10**. In this analysis, to simulate RC bridge piers subjected to reversed cyclic loading, the flexural compression members and flexural tension members are assumed to have the same cross-sectional area. In addition, since the specimen is a cantilever RC bridge pier, two intersecting arch members connecting the loading points at the top of the pier and the opposite pier-footing connections are provided. Here, from the results of pre-analysis already described, the value of t is obtained as 0.20. The applied axial compressive load at the top of the pier is uniformly distributed over the top three nodes.

3.3 Hysteresis characteristic of RC bridge piers

The lateral force-lateral displacement relationships obtained in the experiment and using static lattice model analysis are shown in **Fig. 11**. The experimental result (shown in **Fig. 11 (a)**) shows that the longitudinal reinforcement initially yields on the flexural tension side at the bottom of the RC bridge pier. As lateral displacement gradually increases after reversing the loading direction, the longitudinal reinforcement

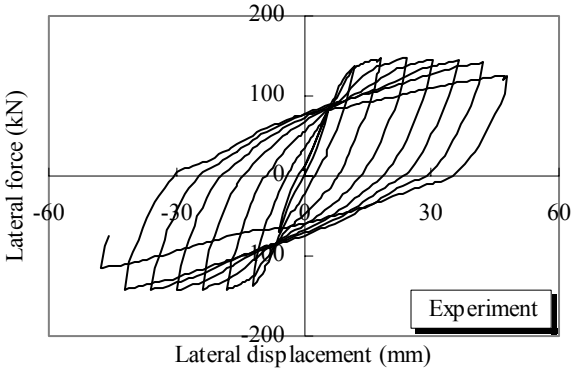

(a) Experiment

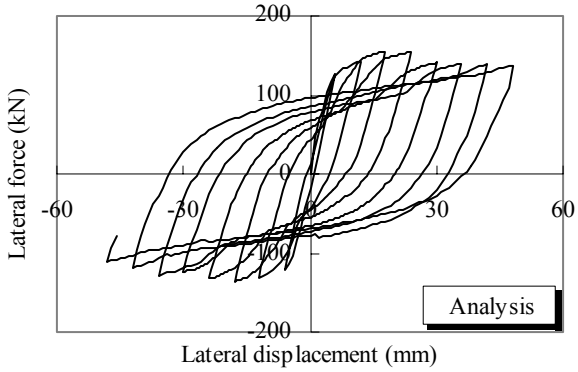

(b) Analysis

Fig. 11 Lateral force and lateral displ ionship (experiment and analysis)

behaves plastically and deforms laterally outwards in a process referred to as buckling. Ultimately, the lateral load-lateral displacement curve reaches the post-peak region accompanied by buckling of the longitudinal reinforcement and spalling of the cover concrete. In the analytical result (shown in **Fig. 11 (b)**) the behavior of the RC bridge pier is found to be close to the experimental result. This comparison of the two results indicates that the newly developed analytical method is applicable to prediction of the stiffness, load carrying capacity, and the cyclic behavior of RC bridge piers after yielding of the longitudinal reinforcement and until the load begins to fall. However, it is also clear that further softening behavior in the post-peak region is not properly predicted by the analysis.

The experimental and analytical results for lateral force and lateral displacement at yielding of the longitudinal reinforcement, as well as the maximum lateral force and the ultimate displacement of the RC bridge pier, are summarized in **Table 2**. In the analysis, the point at which the longitudinal reinforcement yields is defined as when the longitudinal reinforcement strain at the bottom of the pier reaches the yield strain of 2000 μ. This matches the experimental condition. Further, the ultimate displacement is obtained as the lateral displacement at the point when the lateral force corresponds to unity at the yielding of the longitudinal reinforcement in the post-peak region. In the analysis, after yielding of the longitudinal reinforcement, compression softening behavior can be seen in the diagonal concrete member at the base of the pier as the crack width increases perpendicular to the direction of the compressive stress. These analytical results indicate that local behavior causes the post-peak response of a RC bridge pier, and the analytical responses of RC bridge piers are found to be in good agreement with the experimental responses.

Using **Fig. 11**, the experimental and analytical results can be expressed by the envelope curve shown in **Fig. 12**. As noted above, although this analysis predicts the experimental results quite well until the ultimate displacement, some difference between the two can be observed in the large displacement region. This is because buckling of the longitudinal reinforcement and concrete spalling should influence predictions of the behavior of RC bridge piers. That is, in order to correctly predict the behavior of RC bridge piers subjected to large lateral deformations, consideration of reinforcement buckling would be necessary. However, although there is room for improvement in this model, the envelope curves and hysteresis loops for RC bridge piers can be predicted reasonably well up to the ultimate state using the static lattice model presented here.

3.4 Evaluation of failure mode and load-carrying mechanism of RC bridge piers

The load-carrying mechanism is identified from the internal forces by focusing on the stress-strain relationship in one of the lattice components, a diagonal concrete member at the bottom of the pier. The stress-strain relationship of this member, which is marked by the bold line in **Fig. 10**, is shown in **Fig. 13**. In the static lattice model, the compression softening behavior of concrete as proposed by Collins et al. [4] is applied. With respect to one pairing of an intersecting diagonal compression member and a diagonal tension member, it is assumed that the compressive stress capacity of the diagonal members falls as the tensile strain on the members increases. The dashed line in **Fig. 13** represents the stress-strain curve of the

Table 2 Experimental and analytical results of lateral force and lateral displacement (static reversed cyclic loading test and static lattice model analysis)

	Experiment	Analysis
Yield strength (kN)	84.2	116.3
Yield displacement (mm)	6.0	5.0
Maximum lateral force (kN)	148.0	155.6
Ultimate displacement (mm)	42.0	48.0

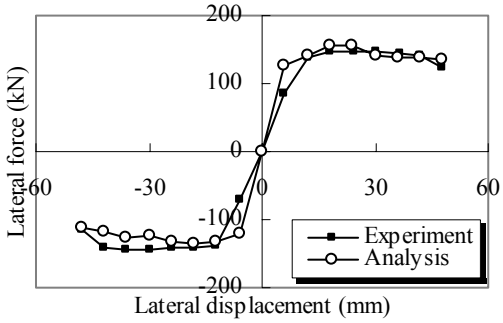

Fig. 12 Envelope curves of lateral force and lateral displacement (experiment and analysis)

uncracked concrete. This figure shows that the compressive stress deteriorates rapidly as diagonal cracks propagate from the pier footing connection. With further loading, these cracks open widely while compressive stress along with the inclined crack falls. Consequently, in the analysis, this compression softening behavior of a strut governs the post-peak behavior of the load-displacement relationship and leads the RC bridge pier to the ultimate state.

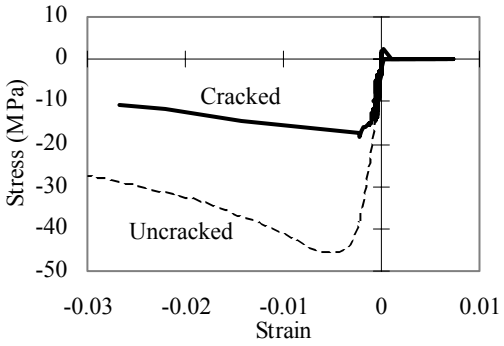

Fig. 13 Stress-strain relationships of concrete in diagonal member

4. NONLINEAR DYNAMIC ANALYSIS OF RC BRIDGE PIERS

4.1 Outlines of target structures

The analytical target selected for dynamic lattice model analysis is a series of shaking table tests [12] on RC bridge piers, as explained below.

The original experiment was carried out on a structural system in which the pier supports a superstructure component consisting of a 393.2 kN beam. The external lateral force acting on the RC bridge pier is the inertial force developed by the beam. The specimen is a cantilever RC bridge pier of rectangular cross-section and with a rigid footing. Details and dimensions of the tested pier are shown in **Fig. 14**. The input ground acceleration is the EW component recorded at Lake Hachiro-gata in Japan during the Nihonkai-Chubu Earthquake of 1983 (**Fig. 15**). The maximum ground acceleration in this motion is 144 gal. In order to bring the predominant period of the ground motion closer to the natural period based on the initial stiffness of the RC bridge pier the time axis of the motion is condensed by half.

The main distinguishing characteristics of this ground motion are the long duration of the principal motion and acceleration peaks that occur at 20 seconds and 50 seconds after the start. A verification based on long-duration ground motion is very useful because it provides different insight than verification based on comparatively large ground motion over a short period, such as experienced during the Hyogo-ken Nanbu Earthquake.

Experiments were carried out on three specimens with different maximum accelerations: 275 gal, 360 gal,

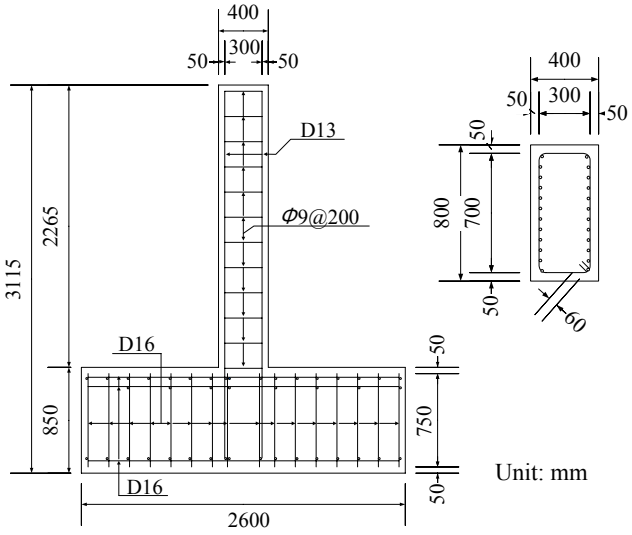

Fig. 14 Specimen details and test setup (shaking table test)

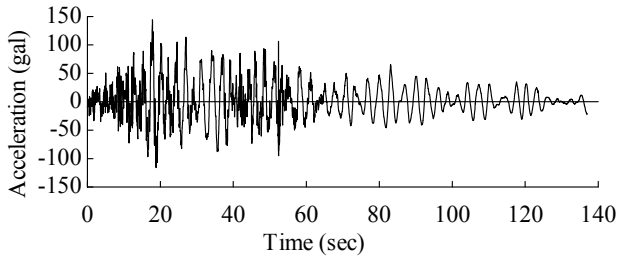

Fig. 15 EW element wave recorded at Lake Hachiro-gata in Japan at Nihonkai-Chubu Earthquake in 1983 (maximum acceleration: 144 gal)

and 402 gal. These are denoted Case-A, Case-B, and Case-C, respectively. As regards the material properties of the specimens, the standard cylindrical compressive strength of the concrete was 27.6 MPa and the yield strength of the longitudinal and transverse reinforcement was 420 MPa.

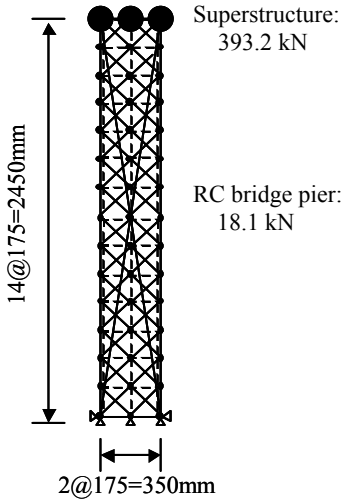

Fig. 16 Dynamic lattice model of RC bridge pier

4.2 Analytical model

The experimental RC bridge pier is modeled into the dynamic lattice model shown in **Fig. 16**. The difference between this and the dynamic lattice model used in a previous study [13] is the confinement effect due to the transverse reinforcement, which is incorporated by applying the stress-strain model proposed by Mander et al. [3]. Moreover, Fukuura's model of reinforcement considering the Bauschinger effect [8], which is manifested as premature yielding of the steel upon reversal of the strain direction, is also employed. The considerations made in applying the constitutive model of each material are also newly improved in this study. The value of t is fixed at 0.10 based on pre-analysis results.

In the dynamic lattice model, the masses of the RC bridge pier and the superstructure are uniformly distributed over all nodal points over the top three nodes, respectively, using the lumped-mass idealization. Damping is introduced into the analysis in the form of viscous forces as Rayleigh damping; the damping coefficient is assumed to be 2.0%.

4.3 Nonlinear dynamic analysis for RC bridge piers

To verify the performance of the lattice model in nonlinear dynamic analysis, experimental results from shaking table tests are adopted for comparison. Further, the seismic behavior of RC bridge piers is evaluated using the dynamic lattice model.

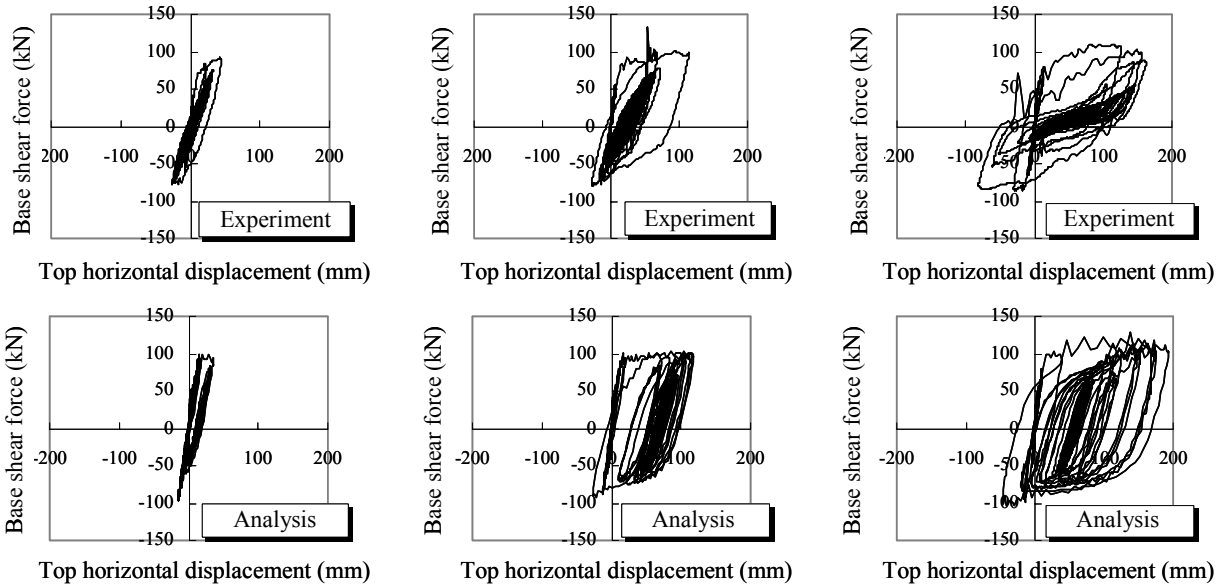

(a) Case-A (275gal) **(b)** Case-B (360gal) **(c)** Case-C (402gal)

Fig. 17 Hysteresis loops of RC bridge piers (experiment and analysis)

Table 3 Experimental and analytical results obtained from shaking table test and dynamic lattice model analysis

	Case-A		Case-B		Case-C	
	Exp.	Ana.	Exp	Ana.	Exp	Ana.
Yield strength (kN)	72.7	90.4	76.1	93.4	79.2	98.5
Yield displacement (mm)	14.1	14.8	15.5	15.5	13.5	15.9
Maximum force (kN)	91.6	99.4	104.3	104.1	110.2	128.8
Maximum displacement (mm)	44.4	34.8	113.6	118.4	163.1	192.6

The hysteresis loops for Case-A, Case-B, and Case-C piers are illustrated in **Fig. 17**, with both experimental results and the analytical results from the dynamic lattice model. In the case of the experimental results, the hysteresis loop is defined as the relationship between the inertial force and the horizontal displacement of the top of the pier. The inertial force can be calculated as the product of the mass of the 393.2 kN beam and the acceleration of the beam. On the other hand, in the case of the analytical results, the relationships between the sum of the restoring forces and the damping forces at the top three nodes and the displacement response at the top of the pier are shown in the figure. The experimental and analytical displacement time histories for the pier top are shown in **Fig. 18**. Moreover, the experimental and analytical responses of the RC bridge pier (yield strength, yield displacement, maximum lateral force and maximum lateral displacement) are tabulated in **Table 3**. In both experiment and analysis, the yield strength and yield displacement are defined as the force and displacement at initial yielding of the longitudinal reinforcement as observed at the bottom of a pier in which the tensile strain of the reinforcement reaches 2,010 μ.

As can be seen in **Fig. 17**, in all the experimental cases the longitudinal reinforcement yielded first. In Case-B, and Case-C, where the input ground acceleration was larger than in Case-A, greater plastic deformation is observed after yielding of the reinforcement. The analytical results demonstrate that these characteristics of RC bridge piers can be predicted using the dynamic lattice model. Furthermore, the dynamic response, such as the maximum lateral force and lateral displacement at the top of RC bridge piers, is evaluated appropriately.

There is, however, a difference between the experimental and analytical results beyond the maximum displacement. In **Fig. 17**, the internal cyclic loop in the experimental results for Case-B indicates a behavior with large vibration amplitude and stiffness lower than the initial stiffness. A comparison of the experimental and analytical results indicates that, beyond the maximum response, the model predicts stiffer behavior and greater amplitude than reality.

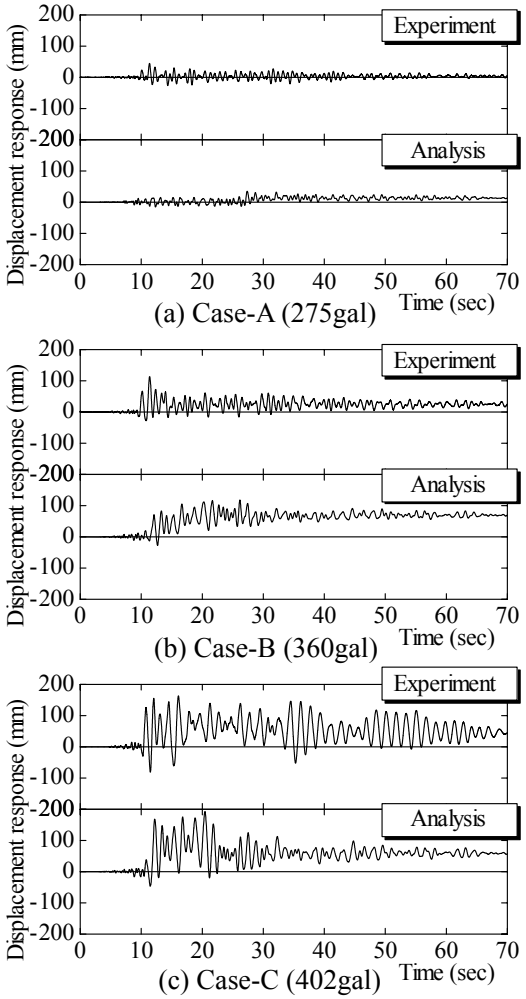

Fig. 18 Displacement time histories of RC bridge piers subjected to three magnitudes of ground motion (experiment and analysis)

Table 4 Material properties and transverse reinforcement ratios

Uniaxial compressive strength of concrete, f_c' (MPa)		38.0					
Yield strength of reinforcement, f_y (MPa)	Longitudinal reinforcement D19	317					
	Transverse reinforcement D6	360					
Transverse reinforcement ratio, r_w (%)		0.00	0.04	0.08	0.12	0.20	0.40

The experimental hysteresis loops for Case-C indicate low stiffness and comparatively less energy dissipation with slight pinching, as shown in **Fig. 17(c)**. On the other hand, the analysis predicts a high capacity for energy dissipation, which contradicts the experimental observation. In particular, it is found that the analytical amplitude of vibrations after 30 seconds is less than the experimental measurements, as shown in **Fig. 18(c)**. This means that the longitudinal reinforcement continues to sustain a large flexural compressive stress despite its buckling behavior. Moreover, this difference arises from assumptions regarding the stiffness of concrete in compression under unloading and reloading conditions. Since the analysis assumes stiffness to be equal to the initial stiffness, the analytical value may be too high. Despite this shortcoming, the dynamic lattice model is able to predict the response of RC bridge piers in the region between yielding of the longitudinal reinforcement and the maximum response very well, although the effects of reinforcement buckling are not taken into consideration.

5. EFFECT OF TRANSVERSE REINFORCEMENT RATIO ON SEISMIC PERFORMANCE OF RC BRIDGE PIERS

5.1 Outlines of analytical procedure

Dynamic lattice analysis is used to model six RC bridge piers with different transverse reinforcement ratios in order to quantify the influence of transverse reinforcement on seismic performance. The analytical targets are cantilever RC bridge piers of rectangular cross section with a height of 2,574 mm. The shape and dimensions of these piers are shown in **Fig. 19**. The material properties are tabulated in **Table 4**. In the table, the transverse reinforcement ratio, r_w, varies from 0.00% (no transverse reinforcement) to 0.40%.

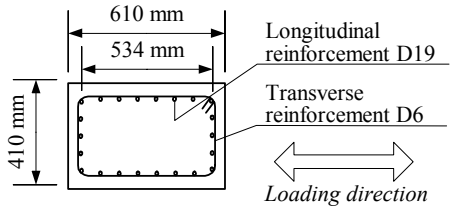

Fig. 19 Cross section of RC bridge pier

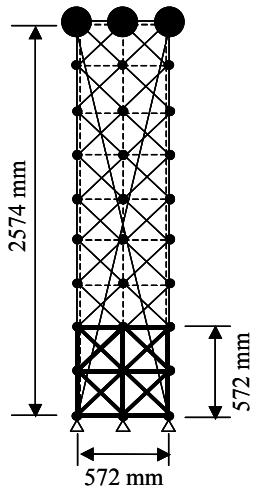

Fig. 20 Dynamic lattice model

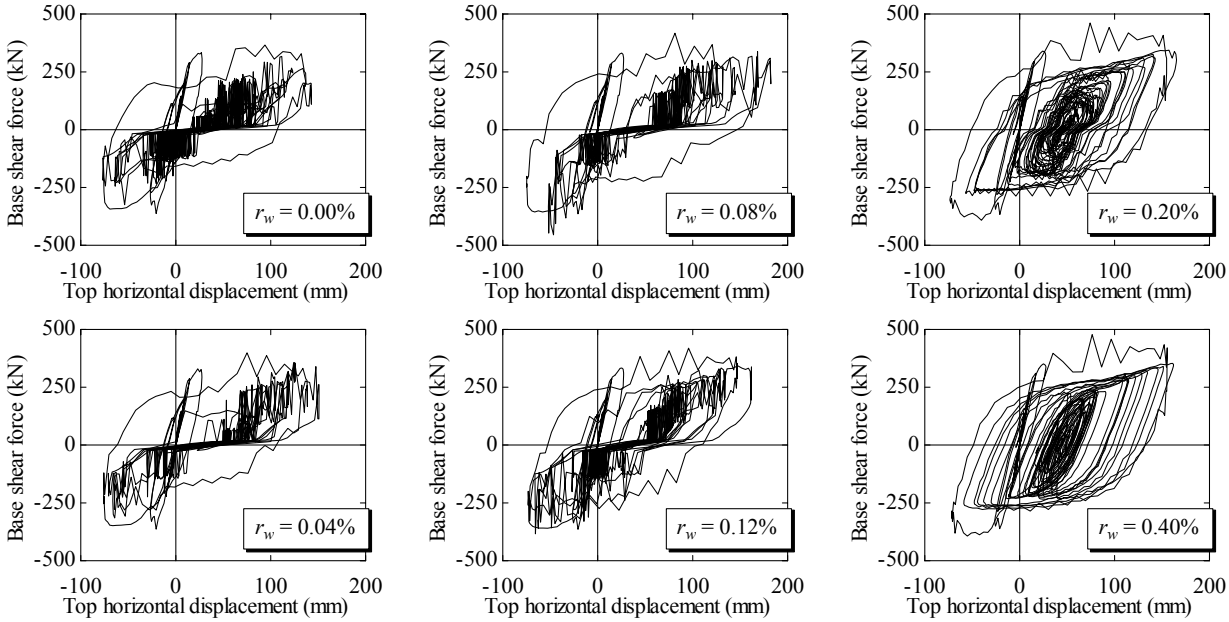

Fig. 21 Hysteresis loops of RC bridge piers with different transverse reinforcement ratios calculated using the dynamic lattice model analysis

The superstructure is modeled as three concentrated masses of 2,000 kN at each of the top three nodes of the pier. The input ground motion is the Nihonkai-Chubu Earthquake motion described earlier and shown in **Fig. 15**. The maximum amplitude of the ground motion is adjusted to 450 gal.

The idealization of the dynamic lattice model is shown in **Fig. 20**. Here, according to pre-analysis, the values of t for the six RC bridge piers are between 0.10 and 0.15, with t rising with increasing transverse reinforcement ratio. This tendency corresponds to observations made in a previous study [11].

5.2 Seismic performance of RC bridge piers with varying transverse reinforcement ratios

The relationship between base shear force and top horizontal displacement as obtained from the analytical model are shown in **Fig. 21**. The maximum response of each pier and the normalized ratio of the response of each pier to that of the pier with no transverse reinforcement (r_w = 0.00%) are shown in **Table 5**. These analytical results confirm that the maximum base shear force increases as the transverse reinforcement ratio is increased. On the other hand, it is also found that the transverse reinforcement ratio has little influence on maximum displacement response within the range of transverse reinforcement ratios investigated in this study.

Table 5 Maximum response of RC bridge piers obtained using dynamic lattice model analysis

Transverse reinforcement ratio, r_w (%)	0.00%	0.04%	0.08%	0.12%	0.20%	0.40%
Maximum force (kN)	366.2 (1.00)	398.5 (1.09)	417.4 (1.14)	419.0 (1.14)	461.7 (1.26)	477.4 (1.30)
Maximum displacement (mm)	142.8 (1.00)	150.9 (1.06)	180.3 (1.26)	162.0 (1.13)	165.3 (1.16)	162.0 (1.13)

Note: The values in parentheses indicate the normalized ratio of the response of each pier to that of the pier with no transverse reinforcement (r_w = 0.00 %).

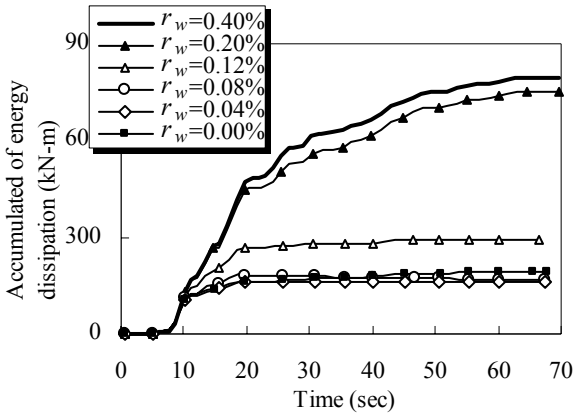

Fig. 22 Accumulated energy dissipation of RC bridge piers with different transverse reinforcement ratios calculated using the dynamic lattice model

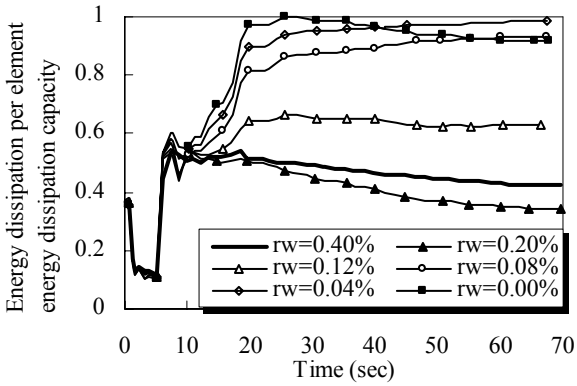

Fig. 23 Ratio of summed energy dissipation in several elements to energy dissipation capacity of RC bridge piers

In **Fig. 21**, however, it is clear that energy dissipation capacity rises as the amount of transverse reinforcement is increased. This influence of transverse reinforcement ratio on energy dissipation capacity will be discussed in the following section.

5.3 Energy dissipation capacity of RC bridge piers

The analytical time histories of cumulative energy dissipation for the six RC bridge piers are shown in **Fig. 22**. This accumulated value of energy dissipation is obtained as the area surrounded by one cycle of the hysteresis loop (in the base shear force versus top horizontal displacement relationship) during the shaking table test. The figure demonstrates that higher cumulative energy dissipation with increasing transverse reinforcement ratio is predicted by the dynamic lattice model. Because of their greater energy dissipation capacity, RC bridge piers with sufficient transverse reinforcement (r_w =0.40%, 0.20%) can be expected to dissipate energy as they are subjected to further seismic loading. On the other hand, RC bridge piers with little or no transverse reinforcement (r_w =0.00%, 0.04%, and 0.08%) cannot be expected to dissipate the energy of subsequent loading because of their limited dissipation capacity.

Next, the distribution of energy dissipation within the pier is verified in terms of the energy dissipated by each element of the lattice model. In this regard, the lattice model comprises several truss elements in which an average stress and average strain relationship is assumed to govern each element. Because of this assumption, the energy dissipated by each element can be easily calculated from the product of the energy dissipated and the element volume, where the energy dissipated in the element is defined as the area closed by the stress-strain relationship for the unloading and reloading curves. The ratio of summed energy dissipation in several elements (one area of focus) to the total energy dissipation capacity of the pier is shown in **Fig. 23** for the six piers. Here, the focus is on a region consisting of two layers from the bottom of the pier (or 1d from the bottom of the pier) as shown by the thick lines in **Fig. 20**. Note that as the value of the ratio in **Fig. 23** approaches 1.0, the greater the energy dissipation in elements in the focused region. In the case of piers with r_w =0.40% and 0.20%, around 40% of all absorbed energy is dissipated in the region of focus. Similarly, the figure is around 60% for the pier with a transverse reinforcement ratio r_w =0.12%. Further, almost all energy is consumed within the 1d region of piers with little or no transverse reinforcement (r_w =0.00%, 0.04%, and 0.08%). Hysteresis energy is dissipated in a zone above the bottom of the pier that becomes wider as the transverse reinforcement ratio is increased. This expansion of the damage zone is confirmed in the analysis. Hence, by taking into the consideration of the energy dissipation in individual elements, the distribution of energy dissipation in an RC bridge pier can be evaluated using the dynamic lattice model. Moreover, this analysis confirms that the damage zone of an RC bridge pier during an earthquake can be quantitatively predicted by evaluating the distribution of energy dissipation.

6. CONCLUSIONS

This study involved the analysis of RC bridge piers subjected to reversed cyclic loading using a static lattice model. Further, results obtained in shaking table tests were compared with analysis using a dynamic lattice model. This nonlinear dynamic analysis was carried out for six RC bridge piers with different transverse reinforcement ratios. The results obtained lead to the conclusions outlined below.

(1) It has been confirmed that the static lattice model analysis considering the nonlinearity of material provides the accurate prediction of the static cyclic response of RC bridge piers until the ultimate stage.

(2) The comparison of analytical results using a dynamic lattice model with the results of shaking table tests demonstrates the applicability of this model to the prediction of the seismic response of RC bridge piers, including the yield strength, the yield displacement, the maximum of the base shear force and the horizontal displacement at the pier top.

(3) It is found that analysis using the static and dynamic lattice models is unable to fully predict the post-peak response of RC bridge piers. A comparison with experimental results shows that it will be necessary to take into consideration buckling of the longitudinal reinforcement if the accuracy of post-peak response predictions is to be improved.

(4) The simulation of RC bridge piers with different transverse reinforcement ratios clarifies that the maximum base shear force rises with increasing transverse reinforcement ratio. On the other hand, the transverse reinforcement ratio is found to have less influence on the maximum response displacement within the range of transverse reinforcement studied. However, by looking at the energy absorbed in individual elements, the distribution of energy dissipated in an RC bridge pier can be accurately evaluated using the dynamic lattice model. Moreover, it is confirmed that the damage zone in an RC bridge pier during an earthquake can be quantitatively predicted by evaluating this distribution of energy dissipation.

Acknowledgements

The authors are extremely grateful to Dr. Shigeki Unjoh and members of the Earthquake Engineering Division of the Public Works Research Institute for their help in providing valuable experimental data on which this study is based. The authors also express their great appreciation to Professor Akie Asada of Tohoku Institute of Technology and Dr. Testuo Takeda of Kajima Technical Research Institute for their assistance in providing the strong-motion data for the 1983 Nihonkai-Chubu Earthquake.

References

[1] Ukon, H., Kohsa, K., Inoue, S., and Yoshizawa, Y.: Non-linear Simulation Analysis Using Fiber Model for Cyclic Loading Experiment of the Standard RC Pier, *Proceedings of JCI*, Vol.17, No.2, pp.463-468, June 1995 (in Japanese).

[2] Niwa, J., Choi, I. C., and Tanabe, T.: Analytical Study on the Shear Resisting Mechanism of Reinforced Concrete Beams, *Journal of Materials, Concrete Structures and Pavements*, JSCE, No.508/V-26, pp.79-88, February 1995 (in Japanese).

[3] Mander, J. B., Priestley, M. J. N., and Park, R.: Theoretical Stress-Strain Model for Confined Concrete, *Journal of Structural Engineering*, ASCE, Vol. 114, No.8, pp.1804-1826, August 1988.

[4] Vecchio, F. J., and Collins, M. P.: The Modified Compression Field Theory for Reinforced Concrete Elements Subjected to Shear, *ACI Journal*, Vol.83, No.2, pp.219-231, March/April 1986.

[5] Uchida, U., Rokugo, K., and Koyanagi, W.: Determination of Tension Softening Diagrams of Concrete by Means of Bending Tests, *Journal of Materials, Concrete Structures and Pavements*, JSCE, No.426/V-14, pp.203-212, February 1991 (in Japanese).

[6] Okamura, H., and Maekawa, K.: Nonlinear Analysis and Constitutive Models of Reinforced concrete, *Gihodo-Shuppan*, May 1991.

[7] Fukuura, N., and Maekawa, K.: Computational Model of Reinforcing Bar under Reversed Cyclic Loading for RC Nonlinear Analysis, *Journal of Materials, Concrete Structures and Pavements*, JSCE, No.564/V-35, pp.291-295, May 1997 (in Japanese).

[8] Kato, B.: Mechanical Properties of Steel under Load Cycles Idealizing Seismic Action, *CEB Bulletin d'Information*, No. 131, pp.7-27, May 1979.

[9] Takemura, K., and Kawashima, K.: Effect of Loading Hysteresis on Ductility Capacity of Reinforced Concrete Bridge Piers, *Journal of Structural Engineering*, JSCE, Vol.43A, pp.849-858, March 1997 (in Japanese).

[10] Ductility Design Subcommittee: *Cyclic Loading Test Data of Reinforced Concrete Bridge Piers*, Earthquake Engineering Committee, JSCE, pp.12-22, March 2001.

[11] Ito, A., Niwa, J., and Tanabe, T.: Evaluation of Ultimate Deformation of RC Columns Subjected to Cyclic Loading Based on the Lattice Model, *Journal of Materials, Concrete Structures and Pavements*, JSCE, No.641/V-46, pp.253-262, February 2000 (in Japanese).

[12] Kawashima, K., and Hasegawa, K.: Experimental Investigation on Nonlinear Seismic Response of Bridge Columns and Accuracy of Equal Energy Assumption, *Journal of Structural Mechanics and Earthquake Engineering*, JSCE, No.483/I-26, pp.137-146, January 1994 (in Japanese).

[13] Ito, A., Niwa, J., and Tanabe, T.: Non-linear Dynamic Analysis of Reinforced Concrete Piers Based on Lattice Model, *Journal of Materials, Concrete Structures and Pavements*, JSCE, No.676/V-51, pp.27-39, May 2001 (in Japanese).